CHARACTERIZATION OF EDGE STRUCTURE AND MISORIENTATION BETWEEN LAYERS OF MICROWAVE PLASMA SYNTHESIZED FEW-LAYER GRAPHENE NANOSHEETS

[1]Jana JURMANOVÁ, [1]Ondřej JAŠEK, [1]Jozef TOMAN, [1]Dalibor VŠIANSKÝ, [1]Pavel SŤAHEL

[1]Faculty of Science – Masaryk University Brno, Brno, Czech Republic, EU, janar@physics.muni.cz

https://doi.org/10.37904/nanocon.2020.3766

Abstract

Topological and edge defects and misalignment of graphene layers in few-layer graphene strongly influence its chemical reactivity and thermal stability. Scanning and transmission electron microscopy and image analysis was used to determine alignment, degree of rotation, between layers in few-layer graphene prepared by decomposition of ethanol in microwave plasma torch at atmospheric pressure. The prepared nanosheets consisted of 1 to 20 layers, with interlayer distance of 0.34 nm, and the main structure was formed by successive growth of individual layers on top of each other. Using FFT, the edges and wrinkles were separated from the graphene layers themselves. The layers were spread out on each one separately and the angles of rotation between them were measured. The rotation angle between layer was from 20 to 30 degrees and the high quality graphene nanosheets, Raman bands 2D/G ratio of 1.6 and D/G ratio of 0.5, exhibited predominantly closed edges and opened edges were mostly found in the layers forming islands on the main structure. Graphene nanosheets remain fully stable in vacuum up to 1000 °C and thermogravimetric analysis showed complete burnout of the sample in synthetic air at 770 °C with more defective sample exhibiting higher weight loss between 400 and 700 °C.

Keywords: Graphene, edge structure, layer orientation, microwave plasma

1. INTRODUCTION

In-plane and edge defects, as well as misalignment of graphene layers have significant impact on many practical applications of few-layer graphene. Freestanding graphene nanosheets can be used as composite filler, anti-corrosive coatings, gas and chemical sensors or light weight and transparent conductors in flexible electronics and displays [1]. High temperature stability under inert or oxidation atmosphere plays a key role in these future key enabling technologies such as batteries for electric transport, flexible electronics and smart building and textile materials. It was also shown recently that twisted graphene with small rotation between layers exhibits superconductivity [2] opening further possible applications in quantum computing and spintronics. Due to the limited size of microwave plasma synthesized graphene nanosheets, from tens to hundreds of nanometers, the structure needs to be stabilized by elimination of free dangling bonds and various types of defects. Formation of curved and closed edges is one of the mechanisms responsible for the stabilization of the structure by minimizing the energy of nanosheet structure [3]. Another way to limit a chemical reactivity is the formation of carbon-hydrogen bonds during the synthesis process either by addition of -CH groups or by reactions with atomic hydrogen. Therefore, the elimination of zero dimensional defects in the graphene structure by optimization of growth conditions further increases the importance of corrugations and edges in the chemical reactivity of freestanding graphene nanosheets. In this work, we investigate structure of edges and misorientation of individual layers in microwave plasma synthesized few-layer graphene nanosheets and their effect on nanosheet's high temperature oxidation.

2. EXPERIMENTAL

Graphene nanosheets were synthesized by decomposition of ethanol in argon carrier gas using dual-channel microwave plasma torch (MPT) at atmospheric pressure. Depending on the deposition conditions two kinds of samples were prepared. High quality graphene (hqG) nanosheets were prepared with central channel flow Qc 500 sccm and 350 W delivered microwave power in laminar flow regime. Defective graphene (dG) nanosheets with high number of defects were synthesized using central channel flow of 920 sccm and 350 W delivered microwave power in unstable gas flow dynamics. In all cases the liquid mass flow rate of ethanol was 45 mg per minute carried by secondary argon gas channel Qs (700 sccm) into reaction chamber. The detailed description of the experimental procedure can be found in our previous publications [4], [5]. Samples were imaged with TESCAN scanning electron microscope (SEM) MIRA3 with Schottky field emission electron gun equipped with Oxford Instruments EDX analyzer. Transmission electron microscopy (TEM) was carried out using JEOL JEM-2100F and FEI Tecai F20 microscope. ImageJ Fiji software was used for determination of nanosheet size and Fast fourier transform (FFT) image analysis. Raman spectroscopy was carried out using HORIBA LabRAM HR Evolution system with 532 nm laser, using 100x objective, and 5% ND filter (500 mW maximum power), 600 grating and 30 s acquisition time in the range from 1000 to 3200 cm^{-1}. Thermogravimetric analysis (TGA) was carried out using a Setaram Setsys Evoluton 1750 instrument. The analyses were conducted in a dynamic air atmosphere (20 $sccm^{-1}$) with a constant heating rate of 5 °C.min^{-1} in the temperature range from 40 to 1000 °C. The obtained data were processed using the Setaram Processing software. The thermal stability of the carbon nanomaterial was investigated as a function of thermal annealing under UHV conditions using thermal desorption spectroscopy (TDS). The samples, graphene powder on Si/SiO_2 substrate were annealed at pressure of 10^{-5} Pa up to 1000 °C with constant heating rate of 10 °C.min^{-1}.

The mass spectrometer Pfeiffer Vacuum Prisma 80 was set in order to follow the evolution of hydrogen and hydrocarbon species in time.

3. SEM AND TEM ANALYSIS OF GRAPHENE NANOSHEETS

Two samples were analyzed: high quality (hqG) and defective (dG) graphene. Both types of samples are prepared in the form of foam formed from nanosheets and individual nanosheets are oriented in various directions (**Figure 1**).

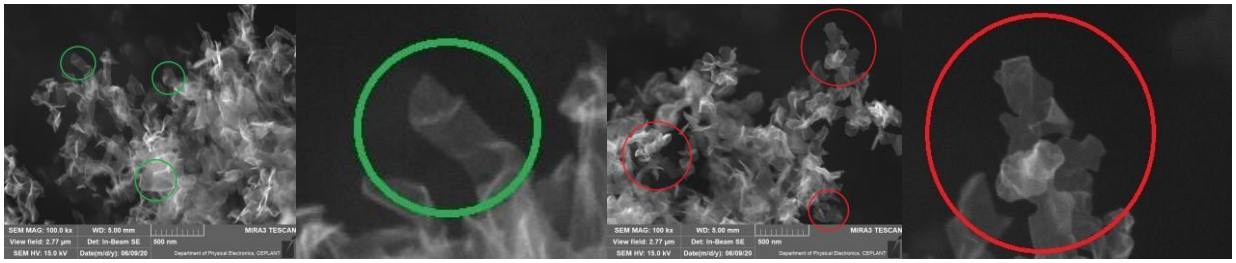

Figure 1 SEM image of hqG and dG nanosheet samples (from left to right). The good sheets are in green circles, the damaged in red.

The individual nanosheets are rectangular in shape with size of several hundreds of nm and it was difficult to distinguish between high-quality and low-quality graphene for the untrained eye. Therefore, it was necessary to evaluate orientation of multilayer structure of nanosheets and whether the sheets have torn edges or not i.e. high number of defects on the structure boundary which would be a sign of poor-quality graphene. The more defective sheets exhibit small changes of contrast in the crystal plane and breaks around the edges. In **Figure 1**, the nanosheets with closed edges are circled in green and the ones with broken ones are circled in red. Detailed images of graphene nanosheets were obtained by high resolution TEM. As can be seen in **Figure 2**, the hqG sample consisted of overlapping graphene layers with closed edges, clean straight lines in

the image. dG sample consisted of a main graphene layer covered with small islands of graphene and closed carbon networks. The edges of the small nanosheets were mostly opened and the main structure edge consisted of opened and closed sections.

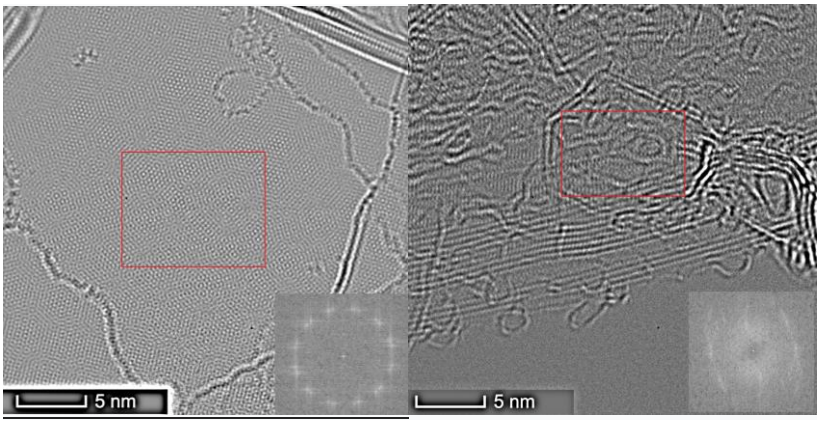

Figure 2 HRTEM image of hqG (left) and dG (right) nanosheet samples. Inset - FFT analysis of multilayer structure

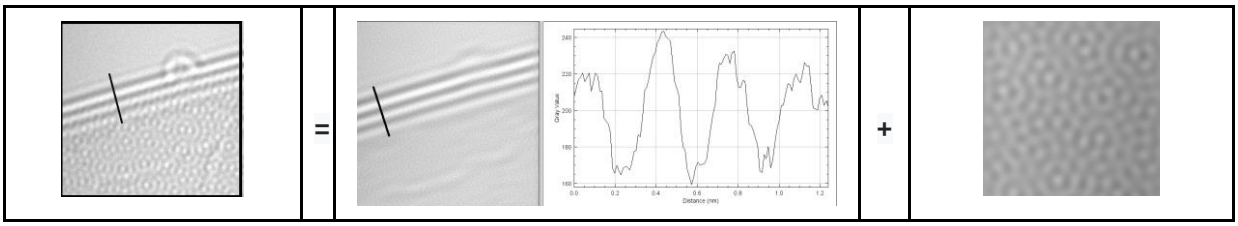

Figure 3 Separation of the edges and wrinkles from the graphene layer itself and determination of distance between graphene layers (0.3 – 0.4 nm)

The FFT (Fast Fourier Transformation) of graphene [6] is a very powerful tool that allows us determination of orientation of individual layers, inset of **Figure 2**, and the separation of an edge from the surface of a layer [7] as shown in **Figure 3**. The FFT of graphene exhibits six-fold symmetry, so the number of dots indicates the number of graphene layers on top of each other. By measuring the angle between the lines connecting the points, that represent different layers, and the center of the shape, it is possible to determine how much these layers are rotated towards each other [8], see **Figure 4**.

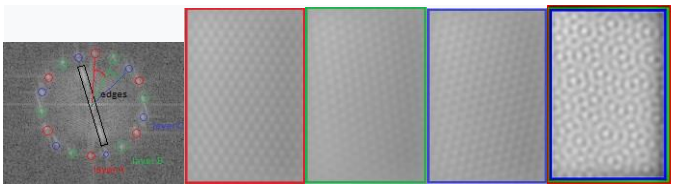

Figure 4 FFT analysis of three-layer graphene (on the Figure 3) and the modeling of the whole layer. The angles between layers are approximately 20 degrees.

The intact edge gives the FFT pattern with the preferred direction (**Figure 5** FFT B, C, D on the left), which indicates the orientation of the edge in space. The defect edge creates a random arrangement in the FFT pattern (bright area inside the circle on FFT A on the left). On the regular edges with a local defect, the FFT pattern is a combination of the above (FFT A,B,C,D on the right) [9]. Such analysis of our nanosheets showed substantially higher number of defects on the edges of dG sample than in case of hqG sample.

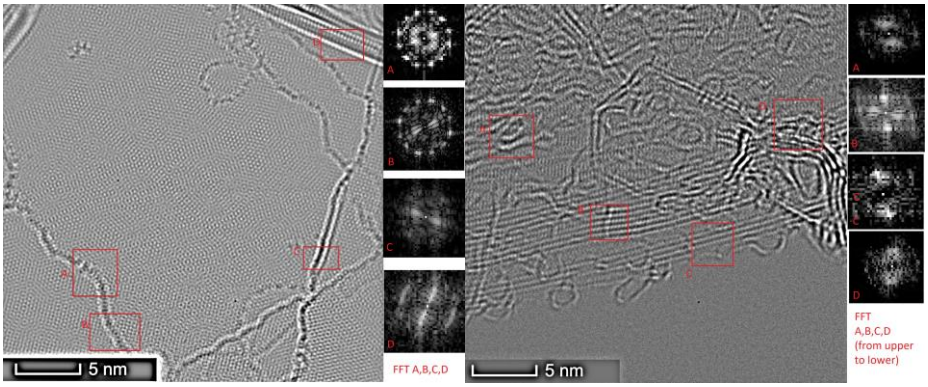

Figure 5 FFT analysis of the edges of hqG (left) and dG (right) graphene nanosheets.

4. RAMAN SPECTROSCOPY OF GRAPHENE NANOSHEETS

To investigate the degree of disorder in the studied samples we compared Raman spectra of synthesized graphene nanosheets (**Figure 6**). Raman spectra of both types of samples consisted of D, G and 2D bands [10] at 1350, 1580 and 2690 cm^{-1}, respectively. The G band is related to the in-plane bond stretching of carbon atoms in crystal structure with sp^2 hybridization and D band is activated in the presence of defects in the hexagonal structure. In our case it was also found in the Raman spectra due to the bending and folding of nanosheets edges, which play an important role in the stabilization of the whole structure. 2D band is highly enhanced in the single layer graphene and with increasing number of layers its intensity decreases and full width half maximum (FWHM) of the 2D peak is increasing, from 30 to 60 cm^{-1}. In our high-quality sample, the 2D/G ratio was 1.6 and FWHM of 2D band was 50 cm^{-1}. In case of more defective sample, the 2D/G ratio decreased to 1.1 and D/G ratio increased from 0.5 to 0.8.

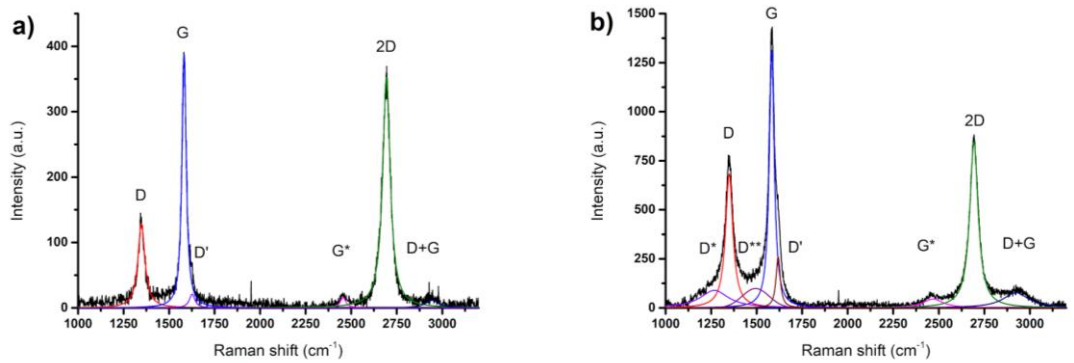

Figure 6 Raman spectra of a) hqG and b) dG nanosheet samples.

Substantial difference was found in the intensity of disorder related bands D* - 1260 cm^{-1}, D** - 1495 cm^{-1} and D´ - 1618 cm^{-1}. These bands are activated in the presence of amorphous phase and opened edges in the nanosheets structure. The intensity of these bands was negligible in the case of hqG sample but in the spectra of dG sample, the (D*+D**+D')/G ratio was 0.8. Except first order Raman bands, second order bands G* at ~2450 cm^{-1} and D+G band at ~2950 cm^{-1} were observed in the measured spectra as well.

5. THERMAL DESORPTION SPECTROSCOPY ANALYSIS

At first, thermal stability of graphene nanosheets was investigated by thermal annealing and mass spectrometry in high vacuum. Measured mass spectra were consistent with expected thermal decomposition of carbon nanostructures. CO and CO_2 molecules and C_2H_xO precursor fragments were observed at

temperatures of 960 °C and 640 °C, respectively. CO and CO_2 were formed by the reaction of carbon and oxygen incorporated into graphene nanosheets structure and residual oxygen in the apparatus. The observed intensity of these compounds was in agreement with the thermodynamic calculations of standard Gibbs energy for reactions of carbon and oxygen [11] where the formation of CO is favored over CO_2 with increasing system temperature. No visible change of the nanomaterial was observed at the whole temperature range and Raman spectroscopy analysis of annealed sample showed no significant variation of either intensity or FWHM of Raman peaks showing good thermal stability of graphene nanosheets in vacuum. Due to the small amount of oxygen, several atomic percent, even more disordered graphene structure did not exhibit any substantial structural changes.

6. THERMOGRAVIMETRY ANALYSIS OF GRAPHENE NANOSHEETS

We further investigated the influence of the amount of disorder on thermal stability of prepared nanosheets in synthetic air at temperature range between 40 and 1000 °C (**Figure 7**). Size of nanosheets and amount of in-plain defects and structure of edge play the main role in the oxidation resistance of carbon nanomaterial. Morgan et al. [12] developed the so-called “shrinking core model”, where the particles with smaller diameter exhibit lower temperature of oxidation. Similarly, nanostructures with lower level of graphitization and higher amount of defects will exhibit lower temperature of combustion, because the point and linear defects in the crystal structure are more susceptible to thermal decomposition by oxidation reaction [13].

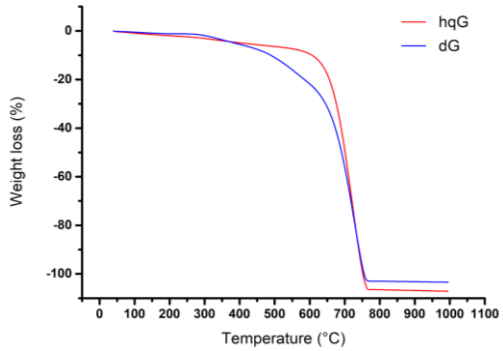

Figure 7 Thermogravimetry analysis of prepared few-layer graphene nanosheets

Overall TGA curve of carbon based materials exhibited several regions. The initial mass loss was occurring around 100 °C and corresponds to the release of water vapors from the carbon particle surface. At higher temperatures between 200 and 300 °C, the thermal decomposition of unstable oxygen-containing functional groups as well as intercalated water release can occur, but this region was negligible in our samples. The graphene based nanomaterial itself begins to combust above 300 °C, where decomposition of light amorphous poly-carbons to carbon dioxide occurs which are easily vaporized as can be seen on the TGA curve of dG sample. At last, gradual decomposition of graphene nanosheets structure itself followed above 600 °C due to the breaking of C-C bond and exothermic reaction between carbon and oxygen formed CO and CO_2. Due to small number of defects and stable nanosheets edges, hqG sample exhibited only the last described region above 650 °C and complete loss of material was observed at 770 °C. Abrupt loss of material at this temperature was consistent with first-order reaction kinetics of simple oxidation reaction. dG sample with higher amount of disorder exhibited loss of material above 300 °C and between 450 and 650 °C, but reached the same temperature of complete weight loss (100 %) at 765 °C.

7. CONCLUSIONS

Orientation and edge structure of individual layers of few-layer graphene prepared by microwave plasma decomposition of ethanol was studied by high resolution electron microscopy. Misorientation of layers was 20°

or more and it was independent of the degree of disorder determined by Raman spectroscopy. Detailed image and FFT analysis of individual nanosheets determined large contributions of opened edges to sample disorder in nanosheets prepared in an unstable gas flow regime. Such nanosheets exhibited higher oxidation rate in air during thermogravimetric analysis with two additional regions related to amorphous and highly disordered carbon.

ACKNOWLEDGEMENTS

This work was supported by The Czech Science Foundation under project 18-08520S and in part by project LM2018097 funded by the Ministry of Education, Youth and Sports of the Czech Republic. We acknowledge CEITEC Nano Research Infrastructure supported by MEYS CR (LM2018110). We would like to thank Jiri Bursik for TEM analysis.

REFERENCES

[1] FERRARI, A. C. et al. Science and technology roadmap for graphene, related two-dimensional crystals, and hybrid systems. *Nanoscale.* 2015, vol. 7, no. 11, pp. 4598–4810.

[2] CAO, Y. et al. Unconventional superconductivity in magic-angle graphene superlattices. *Nature.* 2018, vol. 556, no. 7699, pp. 43–50.

[3] YANG, G., LI, L., LEE, W. B., NG, M. C. Structure of graphene and its disorders: a review. *Sci. Technol. Adv. Mater*. 2018, vol. 19, no. 1, pp. 613–648.

[4] TOMAN, J., JASEK O., SNÍŘER M., KUDRLE V., JURMANOVA, J. On the interplay between plasma discharge instability and formation of free-standing graphene nanosheets in a dual-channel microwave plasma torch at atmospheric pressure. *Journal of Physics D: Applied Physics.* 2019, vol. 52, no. 26. p. 265205.

[5] JASEK, O., TOMAN, J., JURMANOVÁ, J. et al. Study of graphene layer growth on dielectric substrate in microwave plasma torch at atmospheric pressure. *Diamond and Related Materials.* 2020, vol. 105. p. 107798.

[6] YEHLIU, K., VANDER WAL, R. L., BOEHMAN, A. L. Development of an HRTEM image analysis method to quantify carbon nanostructure. *Combustion and Flame.* 2011, vol. 158, no. 9. pp. 1837-1851.

[7] SHEN, Z. et al. Preparation of graphene by jet cavitation. *Nanotechnology.* 2011, vol. 22, no. 36, p. 365306.

[8] ROBERTSON, A. W., WARNER, J. H. Atomic resolution imaging of graphene by transmission electron microscopy. *Nanoscale.* 2013, vol. 5, no. 10, pp. 4079-4093.

[9] WARNER, J. H. et al. Structural transformations in graphene studied with high spatial and temporal resolution. *Nat. Nanotechnol*. 2009, vol. 4, no. 8, pp. 500–504.

[10] DRESSELHAUS, M. S., JORIO, A., SOUZA FILHO, A. G. et al. Defect characterization in graphene and carbon nanotubes using Raman spectroscopy. *Philos. Trans. A Math. Phys. Eng. Sci.* 2010, vol. 368, no. 1932, pp. 5355–5377.

[11] DEMIDOV, A. I. MAKRELOV, I. A. Thermodynamics of Reaction of Carbon with Oxygen. *Russian Journal of Applied Chemistry.* 2005, vol. 78, no. 5. pp. 707–710.

[12] MORGAN, P. A., ROBERTSON, S. D., UNSWORTH, J.F. Combustion studies by thermogravimetric analysis. *Fuel.* 1986, vol. 65, no. 11. pp. 1546–1551.

[13] BOM, D. et al. Thermogravimetric Analysis of the Oxidation of Multiwalled Carbon Nanotubes: Evidence for the Role of Defect Sites in Carbon Nanotube Chemistry. *Nano Letters.* 2002, vol. 2, no. 6. pp. 615–619.